Altered Topological Patterns of Brain Networks in Remitted Late-Onset Depression:
A Resting-State fMRI Study

Zan Wang, MD[a,b,‡]; Yonggui Yuan, MD, PhD[a,c,‡]; Feng Bai, MD[a,b]; Jiayong You, MD[d]; and Zhijun Zhang, MD, PhD[a,b,*]

ABSTRACT

Objective: We aimed to investigate the topological organization of whole-brain networks in patients with remitted late-onset depression (rLOD) and to examine the relationship between topological aberrations and performances on neuropsychological tests.

Method: A total of 33 patients with *DSM-IV*–diagnosed rLOD and 31 healthy control subjects underwent resting-state functional magnetic resonance imaging scans. The whole-brain functional networks were constructed by thresholding Pearson correlation matrices of 90 brain regions, and their topological properties (ie, small-worldness, network efficiency, and nodal efficiency) were analyzed using graph theory–based approaches. Nonparametric permutation tests were further used for group comparisons of topological metrics. The patients were recruited from January to December 2007.

Results: Both the rLOD and control groups showed small-world architecture in the functional brain networks, suggesting a balance between functional segregation and integration. Importantly, the rLOD patients exhibited abnormal global topology in their functional brain networks (ie, increased shortest path length and decreased network efficiency) compared with the healthy controls, implying a less optimal topological organization in rLOD. Moreover, the rLOD patients showed decreased nodal efficiencies, predominantly in the frontal-striatal-occipital regions that are closely associated with the neuropathological changes in LOD. Intriguingly, we showed that the topological aberrations correlated with the neuropsychological performances in the rLOD patients.

Conclusions: These results demonstrate that the topological organization of functional brain networks is disrupted in rLOD and that this disruption may contribute to disturbance in cognitive function in rLOD patients.

J Clin Psychiatry 2016;77(1):123–130
dx.doi.org/10.4088/JCP.14m09344

[a]Neuropsychiatric Institute and Medical School of Southeast University, Nanjing, China
[b]Department of Neurology, Affiliated ZhongDa Hospital of Southeast University, Nanjing, China
[c]Department of Psychosomatics and Psychiatry, Affiliated ZhongDa Hospital of Southeast University, Nanjing, China
[d]Department of Psychiatry, Nanjing Brain Hospital, Nanjing Medical University, Nanjing, China.
‡Drs Wang and Yuan contributed equally to this work.
**Corresponding author:* Zhijun Zhang, Neurologic Department of Affiliated ZhongDa Hospital, Neuropsychiatric Institute and Medical School of Southeast University, Nanjing, Jiangsu 210009, China (janemengzhang@vip.163.com).

Late-onset depression (LOD) is often defined as depression with first onset after the age of 60 years, a commonly used cutoff age-point to divide LOD from early-onset depression (EOD).[1,2] Individuals with LOD have clinical pictures distinctive from those of elders with EOD. For instance, patients with LOD are more likely to have associated medical comorbidity, greater cognitive deficits, and increased risk of developing dementia.[3] Further, longitudinal studies demonstrated persistent cognitive impairment or a significantly elevated incidence of Alzheimer's disease in elderly patients with depression.[4] In this regard, there might be an association between LOD and dementia, as previously shown in the literature.[5] However, the neural correlates of this relationship remain unclear. Neuroimaging studies have shown widely distributed structural and functional abnormalities in patients with LOD.[6–11] These findings strongly suggested "brain network dysfunction" as the best explanatory model for understanding the biological mechanism of LOD.

In this context, researchers have recently begun to use graph-theory analysis (GTA) to examine brain network organization. GTA provides a powerful framework for characterizing topological properties of brain networks (for reviews, see references 12–14). For instance, the normal brain is functionally organized in a small-world fashion (characterized by a high local specialization and a high global integration between brain regions), which supports both segregated and integrated information processing.[15–18] Moreover, such an organization pattern is disrupted in various neuropsychiatric disorders, such as Alzheimer's disease[19–21] and schizophrenia.[22–24] Specifically, in patients with major depressive disorder, several research groups have reported topological alterations in the whole-brain connectome, including a loss of small-worldness and a redistribution of hubs.[25–27] The GTA has also been well conducted to measure brain network properties in elderly depression with inconsistent results. Reductions in small-world characteristics and increased disorganization of brain networks are noticed in depressed elders.[28,29] In contrast, 2 recent studies reported no differences in the global topology of brain networks between elderly patients with depression and healthy control subjects.[30,31]

Multiple factors may account for the inconsistency. One of the most predominant factors is that patients enrolled in previous studies are individuals who have EOD but are now older. Given that the individuals with LOD have clinical pictures distinct from those of the elders with EOD, it is meaningful to recruit patients with LOD when conducting studies in depressed elders. Furthermore, most previous studies included acutely depressed patients and did not provide further insight into

their persistent abnormalities. Therefore, we performed a prospective group study combining resting-state functional magnetic resonance imaging (R-fMRI) and graph-theory approaches to investigate the topological architecture of the intrinsic functional brain connectome in patients with LOD. Specifically, we sought to determine whether remitted LOD (rLOD) disrupts the topological organization of the whole-brain functional network and, if so, whether those topological abnormalities are associated with the clinical or behavioral variables.

Clinical Points

- Neuropsychological impairment is a key feature of late-onset depression (LOD) and remains after clinical recovery. However, the neurobiological mechanism underlying the cognitive impairment in remitted LOD (rLOD) remains unclear.
- The topological organization of functional brain networks is disrupted in rLOD, and this disruption may contribute to cognitive deficits in rLOD patients.

METHOD

Participants

The study recruited 64 older, naturally right-handed Han Chinese participants, including 33 patients with *DSM-IV*–diagnosed rLOD and 31 healthy control subjects, from January to December 2007. The detailed inclusion and exclusion criteria are described in eAppendix 1 at PSYCHIATRIST.COM. All participants underwent comprehensive neuropsychological assessments, including auditory verbal learning test–20 minute delayed recall (AVLT-DR),[32] Rey-Osterrieth complex figure test (CFT)[33] and its 20 minute–delayed recall (CFT-DR),[33] clock-drawing test (CDT),[34] Trail-Making Tests A and B (TMT-A and TMT-B),[35] digit span test (DST),[36] and symbol digit modalities test (SDMT).[37] The Research Ethics Committee of Affiliated ZhongDa Hospital, Southeast University, approved the study, and written informed consent was obtained from all participants.

Imaging Acquisition

All subjects were scanned using a General Electric 1.5 Tesla scanner (General Electric Medical Systems, USA) with a homogeneous birdcage head coil (eAppendix 1). During the imaging acquisition, participants were asked to lie quietly in the scanner with their eyes closed. The scan lasted for 426 seconds and included 142 volumes for each participant.

Imaging Preprocessing

Imaging preprocessing was carried out using the Statistical Parametric Mapping software (SPM8, http://www.fil.ion.ucl.ac.uk/spm; eAppendix 1) and included the removal of the first 10 volumes, correction for timing differences and motion effects, spatial normalization to the Montreal Neurologic Institute space, linear detrend, temporal band-pass filtering (0.01–0.1 Hz), and regression of nuisance signals involving 6 head motion parameters, global mean signal, cerebrospinal fluid signal, and white matter signal.

Network Construction

To construct the functional brain network, the images of each brain were first parcellated into 90 regions of interest (ROIs; Supplementary eTable 1) using the automated anatomically labeling atlas. To measure interregional resting-state functional connectivity, Pearson correlation coefficients between any pair of ROIs were calculated, thus generating a 90×90 correlation matrix for each subject. Each absolute correlation matrix was then thresholded into a binary matrix with a fixed sparsity level, S (defined as the number of edges in a graph divided by the maximum possible number of edges of the graph). As there is no gold standard for a single threshold, we thresholded each absolute correlation matrix repeatedly over a wide range of sparsity levels ($10\% \leq S \leq 34\%$) at an interval of 0.01. The details on the network construction can be found in eAppendix 1 and Supplementary eFigure 1.

Network Analysis

For the constructed brain networks at each sparsity threshold, we calculated both global and regional network measures. The global measures included (1) small-world parameters[38] involving clustering coefficient (C_p), characteristic path length (L_p), normalized clustering coefficient (γ), normalized characteristic path length (λ), and small-worldness (σ); and (2) network efficiency[39] involving local efficiency (E_{loc}) and global efficiency (E_{glob}). To determine the nodal (or regional) characteristics of the brain networks, we computed the nodal efficiency (E_{nodal}).[40] For a recent review on uses and interpretations of these network measures, see Rubinov and Sporns[41] and eAppendix 1. Moreover, we also calculated the area under the curve (AUC)[27] for each network metric, which provides a summarized scalar for topological characterization of brain networks independent of single threshold selection.

Statistical Analysis

Behavioral data. To increase statistical power by reducing random variability, as previously introduced,[42] we grouped the neuropsychological tests into 4 cognitive domains (ie, episodic memory, visuospatial skills, processing speed, and executive function) and transformed the raw scores into 4 composite z scores. The details on the composite score analysis were described in eAppendix 1.

Group differences were investigated using a multivariate general linear model, with age, gender, and years of education as covariates. Furthermore, LOD patients show cognitive deficits mainly in the processing speed and executive domains.[43] So, in order to examine whether multiple deficits are mediated by deficits in executive function or processing speed, analyses were repeated with the z scores

Table 1. Demographic Data and Cognitive Performance Results[a]

Item	Patients With rLOD	Healthy Controls	P Value
Demographic data			
Participants, n	33	31	…
Age, y	68.2 ± 4.5	71.2 ± 4.1	.007[b]
Gender, male/female, n	13/20	15/16	.469[c]
Education, y	14.4 ± 1.8	14.7 ± 2.7	.597[b]
Age at onset, y	65.1 ± 4.3	…	…
Duration of illness, y	3.1 ± 1.2	…	…
Neuropsychological test data			
HDRS[e]	1.12 ± 1.0	0.71 ± 0.9	.152[d]
MMSE[e]	28.8 ± 2.0	28.4 ± 1.3	.895[d]
Episodic memory	−0.23 ± 0.80	0.24 ± 0.67	.009[d]
AVLT-DR	−0.36 ± 1.06	0.39 ± 0.78	.001[d]
CFT-DR	−0.09 ± 1.07	0.10 ± 0.92	.520[d]
Executive function	−0.27 ± 0.90	0.29 ± 0.74	.001[d]
DST	−0.14 ± 1.08	0.15 ± 0.90	.118[d]
TMT-B (second)	−0.40 ± 0.93	0.43 ± 0.89	.000[d]
Processing speed	−0.36 ± 0.93	0.39 ± 0.75	.000[d]
SDMT	−0.32 ± 1.10	0.34 ± 0.76	.000[d]
TMT-A (second)	−0.41 ± 0.95	0.43 ± 0.87	.000[d]
Visuospatial skills	−0.24 ± 0.91	0.26 ± 0.35	.004[d]
CFT	−0.28 ± 1.31	0.30 ± 0.27	.003[d]
CDT	−0.20 ± 1.25	0.21 ± 0.59	.221[d]

[a]Data are presented as mean ± SD unless otherwise noted.
[b]Independent-sample *t* test.
[c]χ^2 test.
[d]Analysis of covariance.
[e]See reference 45 for the HDRS and reference 46 for the MMSE.
Abbreviations: AVLT-DR = auditory verbal learning test–delayed recall, CDT = clock-drawing test, CFT-DR = Rey-Osterrieth complex figure test–delayed recall, DST = digit span test, HDRS = Hamilton Depression Rating Scale, MMSE = Mini-Mental State Examination, rLOD = remitted late-onset depression, SDMT = Symbol Digit Modalities Test, TMT = Trail-Making Test.
Symbol: … = not applicable.

of the executive function or processing speed included as an additional covariate.

Network metrics. Between-group differences in topological attributes (both global and regional measures) were investigated by nonparametric permutation tests[44] (eAppendix 1). Of note, before the permutation tests, multiple linear regression analyses were applied to remove the confounding effects of age, gender, and years of education for each network metric.

Brain-behavioral relationship. To investigate the clinical relevance of altered brain network topologies in the rLOD group, we correlated neuropsychological measures with the topological properties at a fixed sparsity (ie, $S = 0.17$, corresponding to the maximal between-group difference in the global efficiency). Partial correlation analysis was used, controlling for age, gender, yeas of education, and duration of illness as confounding variables. Bonferroni correction for multiple comparisons was used with the significance level set at $P < .0125$ ($P = .05/4$ composite scores).

RESULTS

Demographic Information and Cognitive Performance

Demographic information and clinical evaluations for all participants are shown in Table 1 and Supplementary eTable 2. Although no significant between-group differences were found in the education and gender distribution, the 2 groups were not matched for age (it should be noted that the age effect was removed in all of the following neuropsychological and network analyses).

The rLOD group performed significantly worse than the control group in episodic memory ($P = .009$), executive function ($P = .001$), processing speed ($P < .001$), and visuospatial skills ($P = .004$). However, significant differences in episodic memory and visuospatial skills did not survive with the addition of executive function ($P = .227$, $P = .077$) or processing speed ($P = .535$, $P = .211$) as a covariate. Differences in processing speed remained significant after covarying for executive function ($P = .011$), but differences in executive function did not survive after covarying for processing speed ($P = .439$).

rLOD-Related Alterations in Small-World Properties

Over the entire range of sparsity, functional brain networks of both rLOD and healthy control groups had higher clustering coefficients but almost identical characteristic path lengths in comparison with comparable random networks (Figure 1C–1E), which are typical features of small-worldness.

Despite common small-world architecture, statistical analyses further revealed significant differences in both small-world parameters and network efficiency between rLOD patients and healthy controls (Figure 1). Compared to healthy controls, the rLOD patients showed higher L_p values over a wide range of sparsity ($10\% \le S \le 34\%$). No significant between-group differences were found in the C_p, γ, λ, and σ over the entire range of sparsity. As to network efficiency, the functional brain networks of the rLOD group demonstrated decreased global efficiency E_{glob} and local efficiency E_{loc} compared with those of healthy controls. Further statistical comparisons revealed that there were significant differences ($P < .05$) in global and local efficiency at a range of sparsity ($13\% \le S \le 34\%$ and $16\% \le S \le 28\%$, respectively). Moreover, compared with healthy controls, the rLOD patients demonstrated significantly larger area under the L_p ($P = .02$) curve and smaller area under the E_{loc} ($P = .03$) and E_{glob} ($P = .03$) curves.

rLOD-Related Alterations in Regional Efficiency

To further reveal the influence of this disorder on nodal characteristics of the brain networks, the between-group difference in nodal efficiency was tested at the sparsity of 0.17 corresponding to the maximal between-group difference in the global efficiency. Compared with healthy controls, the rLOD patients showed a widespread reduction in nodal efficiency in many cortical and subcortical regions (permutation with 10,000 tests, corrected for $N_{node} = 90$ multiple comparisons with false positive correction $P < (1/N_{node}) = .011$), including 5 frontal regions (left orbit part of superior frontal gyrus, left opercular part of inferior frontal gyrus, left orbit part of inferior frontal gyrus, right anterior cingulate gyrus, and left rolandic operculum), left insula, 2 occipital regions (left calcarine fissure and surrounding

Figure 1. Group Differences in Global Measures of Functional Brain Networks Quantified Between rLOD and HC Groups[a]

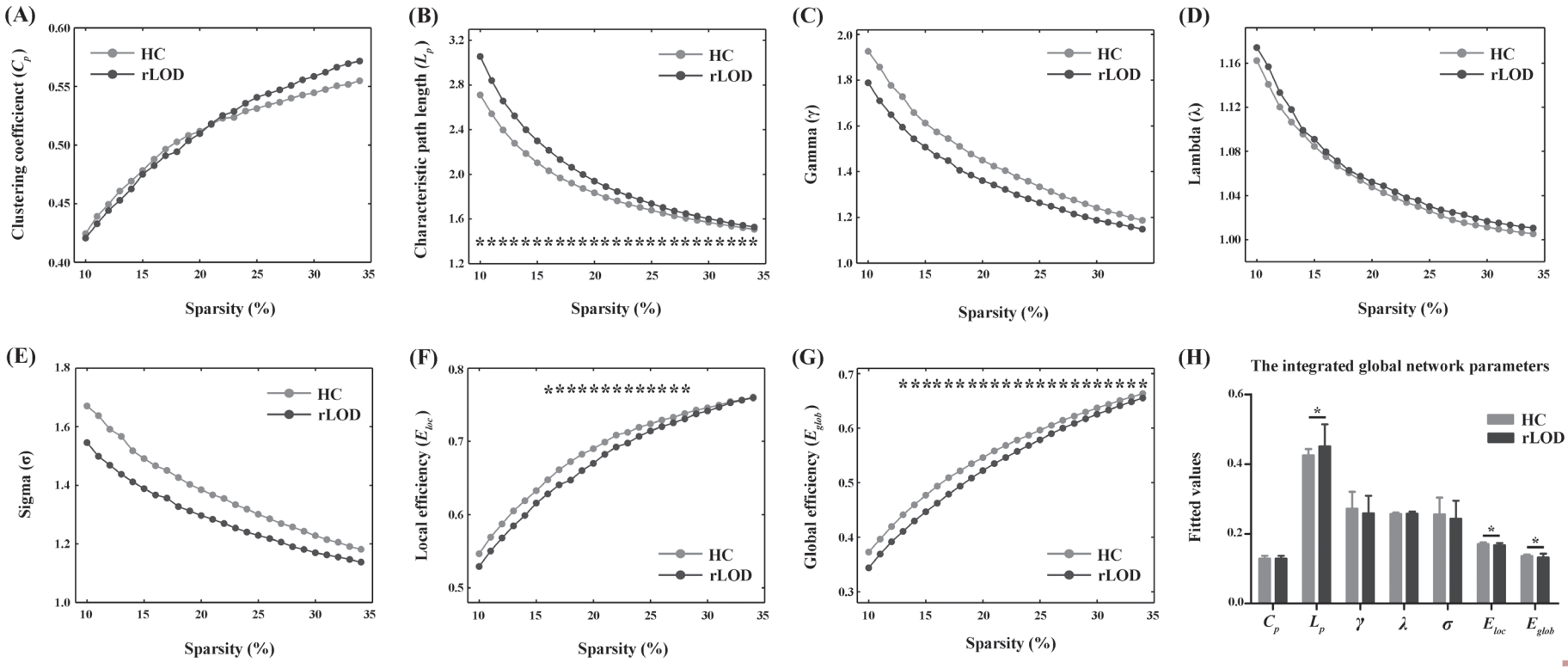

[a](A) Clustering coefficient C_p, (B) characteristic path length L_p, (C) gamma γ, (D) lambda λ, (E) sigma σ, (F) local efficiency E_{loc}, and (G) global efficiency E_{glob} of the rLOD and healthy control groups as a function of sparsity thresholds; (H) between-group differences in the integrated global network parameters. Asterisks (*) indicate when the difference between the rLOD and HC groups is significant.

Abbreviations: HC = healthy control, rLOD = remitted late-onset depression.

It is illegal to post this copyrighted PDF on any website.

Figure 2. Brain Regions Showing Abnormal Nodal Efficiency in Brain Functional Networks[a]

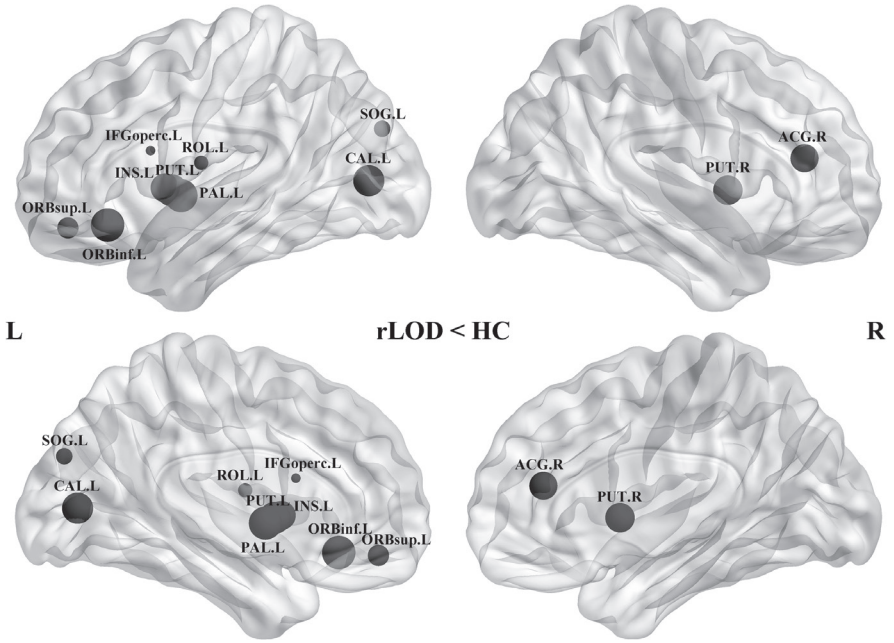

[a]Nodes indicated by shaded circles show the regions that have reduced efficiency in rLOD patients versus controls. The node sizes indicate the significance of between-group differences in the regional efficiency.
Abbreviations: HC = healthy control, L = left, R = right, rLOD = remitted late-onset depression. For the abbreviations of the nodes, see Supplementary eTable 1.

cortex and superior occipital gyrus) and 3 subcortical regions (bilateral putamina and left pallidium) (Figure 2).

Relationships Between Topological Properties and Neuropsychological Measures

We next examined the relationships of the network metrics and the neuropsychological performances. No significant correlations between the global network metrics and the composite *z* scores for cognitive domains were found in the rLOD group. For nodal characteristics, we examined only the nodes with significant between-group differences. Within the rLOD group, nodal efficiency of the left putamen correlated significantly with the episodic memory ($r = 0.543$, $P = .002$) and processing speed ($r = 0.447$, $P = .012$) scores (Figure 3). In addition, we also investigated the relationships between network metrics and the raw scores of each test in the rLOD group (Supplementary eFigure 2). The AVLT-DR scores correlated with the global efficiency ($r = 0.482$, $P = .008$) and absolute path length ($r = -0.466$, $P = .011$). Nodal efficiency of the left putamen correlated positively with the CFT scores ($r = 0.546$, $P = .002$), CFT-DR scores ($r = 0.460$, $P = .010$), SDMT scores ($r = 0.471$, $P = .009$), and AVLT recognition scores ($r = 0.469$, $P = .009$).

DISCUSSION

This study is the first, to our knowledge, to investigate the topological properties of functional brain networks in patients with rLOD using the R-fMRI. Our main findings are as follows: (1) the global topological organization of functional brain networks in rLOD patients was significantly disrupted as indicated by abnormal small-world properties and topological efficiency; (2) the regional characteristics (nodal efficiency) were altered in rLOD patients predominantly in the frontal-striatal-occipital areas; and (3) these abnormal network metrics correlated with the cognitive performances in the rLOD patients. These results suggest a disruption of whole-brain topological organization of the function connectome in rLOD and advance our current understanding of the neurobiological mechanism underlying the cognitive dysfunction in patients with rLOD.

Neuropsychological Impairment in rLOD

Neuropsychological impairment is a key feature of elderly depression and remains after clinical recovery.[47–49] In the current study, we investigated the pattern of neuropsychological impairment in rLOD and found that the rLOD patients performed worse across multiple neuropsychological domains. The finding is consistent with earlier reports that remitted depression had persistence of cognitive impairment.[50,51] Furthermore, inclusion of processing speed as an additional covariate was sufficient to reduce deficits in all other neuropsychological domains to nonsignificant levels, while deficits in processing speed could not be fully accounted for by impaired executive function. Overall, processing speed appears to represent an important cognitive deficit in rLOD, which might contribute to deficits in other neuropsychological domains. Further

Figure 3. Scatter Plots of Regional Nodal Efficiency and Cognitive Performance in rLOD Patients[a]

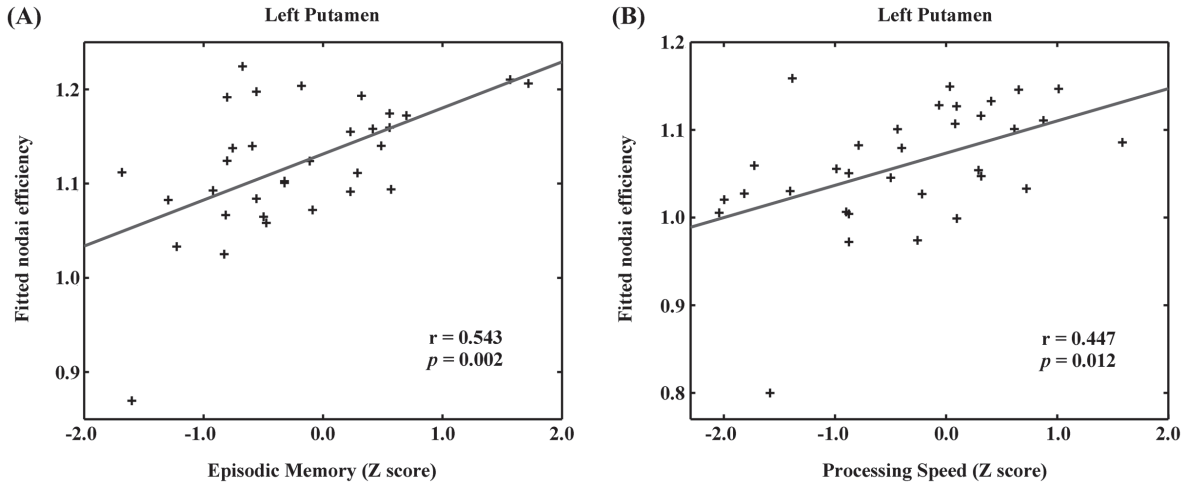

[a]Nodal efficiency of the left putamen correlated positively with the (A) episodic memory and (B) processing speed scores.
Abbreviation: rLOD = remitted late-onset depression.

studies using a more comprehensive neuropsychological battery of tests are warranted to validate this finding.

Disrupted Efficient Small-World Characters in rLOD

The human brain is a complex, interconnected system with an economical, small-world architecture. Functional segregation and integration are 2 major organizational principles of the human brain. In other words, an optimal brain requires an optimal balance between local specialization and global integration of brain functional activity.[52] Within a network, small-worldness enables high efficiency of both specialized and integrated processing.[38] In this study, we found that both rLOD patients and healthy controls showed efficient small-world topology in whole-brain functional networks. This finding is consistent with previous network studies based on different imaging techniques (for reviews, see references 13 and 53).

Although both the rLOD and control groups had economical small-world properties as elucidated earlier, the topology of the rLOD group was altered compared to the control group. The rLOD patients showed an increased path length in their brain networks as compared with healthy controls, whereas there were no significant differences in local clustering. Likewise, network efficiency analysis revealed abnormal small-world organization in the rLOD group, as characterized by reduced global and local efficiency. These findings are consistent with those of previous neuroimaging studies using graph analysis to study depression in elderly individuals.[28,29] Given that the small-world model reflects an optimal balance between local specialization and global integration, these results indicate a disturbance of the normal balance in functional brain networks of rLOD patients. Specifically, the global efficiency reflects the information transfer between remote regions and is mainly associated with long-range connections. The local efficiency is predominantly related to the short-range connections between neighboring regions. Further, short path lengths ensure interregional effective integrity or prompt transfer of information in brain networks, which constitutes the basis of cognitive processes.[54] So, the disease-related increases in the absolute path length and decreases in the network efficiency may be attributable to disconnections between brain regions.

Our results can be supported by many previous studies. Many diffusion tensor imaging studies provided direct evidence for disrupted structural integrity in various white-matter tracts in LOD patients,[6,7] even when the depressive symptom remitted.[11,55] Moreover, recent R-fMRI studies also showed abnormal functional integrity in rLOD.[10,56] More importantly, the present study revealed that the altered global network metrics (ie, L_p and E_{glob}) correlated with the cognitive performance (ie, AVLT-DR scores) in rLOD patients, indicating their potential in characterizing how network disorganization can affect cognitive function associated with disease processes. Together, our finding of loss of small-world characteristics in rLOD reflects a less optimal topological organization in functional brain networks, thus providing evidence that rLOD is a disorder with disrupted neuronal network organization and deficient cognitive processing.

Disrupted Nodal Efficiency in the Functional Brain Networks in rLOD

The nodal efficiency measures the extent of connectivity of a node to all other nodes, likely indicating the importance of a nodal region in the whole brain network.[40] In our study, the frontal-striatal-occipital areas showed decreased nodal efficiency in patients with rLOD, indicating a diminished role of these regions in the functional brain network in rLOD patients.

The rLOD-related decreases in nodal efficiencies were observed in the frontal-striatal-occipital areas that were, in general, concerned in LOD studies. Frontostriatal

dysfunction is a primary hypothesis for the neurocognitive changes of depression in late life. Cognitive assessment in elderly individuals with depression shows a pattern of impairment in executive function and processing speed, also suggestive of dysfunction of frontal and striatal cognitive circuits.[57] Numerous studies have shown that elderly depressed individuals have higher rates (compared with well-matched controls) of gray and white matter brain structural changes affecting frontal and subcortical areas.[58–61] In the resting state, these frontostriatal areas also exhibited abnormal activity[62] and functional connectivity[9] in patients with LOD. Importantly, nodal efficiency of left putamen correlated significantly with the cognitive performances (ie, episodic memory and processing speed scores) in the rLOD patients, suggesting that the abnormal nodal efficiency of left putamen might be involved in the psychopathology and pathophysiology of cognitive dysfunction in rLOD. Overall, these previous findings and our results provide evidence for both structural and functional rLOD-related abnormalities in the frontostriatal areas. Moreover, reduced regional efficiencies were also observed in the occipital cortex regions. Many previous studies have demonstrated that the occipital regions exhibited depression-related abnormalities in the gray matter morphology,[63,64] white matter integrity,[11] and functional interactions.[9,27] Together, our results suggest that the abnormalities in the frontal-striatal-occipital areas might influence information transmission and functional integration for rLOD patients.

Methodological Issues

Several issues need to be further addressed. First, this study was a cross-sectional investigation at a single time point and had a relatively small sample size. Replication of these findings in a large cohort will be necessary for validation. Second, given that all patients were depression-free in the present study, these findings may reflect features that are either a consequence of the previous disease or are a constituent part of the brain organization in subjects vulnerable to LOD. Third, given that all patients have received various antidepressant treatments, the results could not exclude a potential medication effect. Fourth, the present 2 groups were not matched for age, although the age effect was removed in all of the network analyses. Therefore, these data should be interpreted with caution. Finally, a recent study[65] showed that functional brain network topological metrics could be used as effective features to distinguish major depression patients from healthy controls, suggesting that the topological network metrics could serve as biomarkers of depression. With regard to depression in elderly individuals, further studies are important to examine whether the topological network metrics could be used to aid in differential diagnosis of LOD compared with other late-life groups.

Submitted: June 24, 2014; accepted February 26, 2015.

Potential conflicts of interest: None of the authors have a conflict of interest relevant to the publication of this article.

Funding/support: This work was partly supported by the National Natural Science Foundation of China (81171021, 91132727, 81371488, and 81420108012) and the Key Program for Clinical Medicine and Science and Technology: Jiangsu Province Clinical Medical Research Center (BL2013025).

Role of the sponsor: The funding agencies of this research did not have direct influence over the collection, analysis, or interpretation of data.

Acknowledgment: The authors thank all participants.

Supplementary material: Available at PSYCHIATRIST.COM.

REFERENCES

1. Brodaty H, Cullen B, Thompson C, et al. Age and gender in the phenomenology of depression. *Am J Geriatr Psychiatry*. 2005;13(7):589–596.
2. Brodaty H, Luscombe G, Parker G, et al. Early and late onset depression in old age: different aetiologies, same phenomenology. *J Affect Disord*. 2001;66(2–3):225–236.
3. Ballmaier M, Narr KL, Toga AW, et al. Hippocampal morphology and distinguishing late-onset from early-onset elderly depression. *Am J Psychiatry*. 2008;165(2):229–237.
4. Wilson RS, Barnes LL, Mendes de Leon CF, et al. Depressive symptoms, cognitive decline, and risk of AD in older persons. *Neurology*. 2002;59(3):364–370.
5. Schweitzer I, Tuckwell V, O'Brien J, et al. Is late onset depression a prodrome to dementia? *Int J Geriatr Psychiatry*. 2002;17(11):997–1005.
6. Dalby RB, Frandsen J, Chakravarty MM, et al. Correlations between Stroop task performance and white matter lesion measures in late-onset major depression. *Psychiatry Res*. 2012;202(2):142–149.
7. Guo W, Liu F, Xun G, et al. Disrupted white matter integrity in first-episode, drug-naive, late-onset depression. *J Affect Disord*. 2014;163:70–75.
8. Hwang JP, Lee TW, Tsai SJ, et al. Cortical and subcortical abnormalities in late-onset depression with history of suicide attempts investigated with MRI and voxel-based morphometry. *J Geriatr Psychiatry Neurol*. 2010;23(3):171–184.
9. Yue Y, Yuan Y, Hou Z, et al. Abnormal functional connectivity of amygdala in late-onset depression was associated with cognitive deficits. *PLoS ONE*. 2013;8(9):e75058.
10. Wu D, Yuan Y, Bai F, et al. Abnormal functional connectivity of the default mode network in remitted late-onset depression. *J Affect Disord*. 2013;147(1–3):277–287.
11. Yuan Y, Zhang Z, Bai F, et al. White matter integrity of the whole brain is disrupted in first-episode remitted geriatric depression. *Neuroreport*. 2007;18(17):1845–1849.
12. Micheloyannis S. Graph-based network analysis in schizophrenia. *World J Psychiatry*. 2012;2(1):1–12.
13. Sporns O. Structure and function of complex brain networks. *Dialogues Clin Neurosci*. 2013;15(3):247–262.
14. Tijms BM, Wink AM, de Haan W, et al. Alzheimer's disease: connecting findings from graph theoretical studies of brain networks. *Neurobiol Aging*. 2013;34(8):2023–2036.
15. Hagmann P, Kurant M, Gigandet X, et al. Mapping human whole-brain structural networks with diffusion MRI. *PLoS ONE*. 2007;2(7):e597.
16. He Y, Chen ZJ, Evans AC. Small-world anatomical networks in the human brain revealed by cortical thickness from MRI. *Cereb Cortex*. 2007;17(10):2407–2419.
17. Salvador R, Suckling J, Coleman MR, et al. Neurophysiological architecture of functional magnetic resonance images of human brain. *Cereb Cortex*. 2005;15(9):1332–1342.
18. Stam CJ. Functional connectivity patterns of human magnetoencephalographic recordings: a 'small-world' network? *Neurosci Lett*. 2004;355(1–2):25–28.
19. Brier MR, Thomas JB, Fagan AM, et al. Functional connectivity and graph theory in preclinical Alzheimer's disease. *Neurobiol Aging*. 2014;35(4):757–768.
20. He Y, Chen Z, Evans A. Structural insights into aberrant topological patterns of large-scale cortical networks in Alzheimer's disease. *J Neurosci*. 2008;28(18):4756–4766.
21. Seo EH, Lee DY, Lee JM, et al. Whole-brain functional networks in cognitively normal, mild cognitive impairment, and Alzheimer's disease. *PLoS ONE*. 2013;8(1):e53922.
22. Lynall ME, Bassett DS, Kerwin R, et al. Functional connectivity and brain networks in schizophrenia. *J Neurosci*. 2010;30(28):9477–9487.
23. Zhang Y, Lin L, Lin CP, et al. Abnormal topological organization of structural brain networks in schizophrenia. *Schizophr Res*. 2012;141(2–3):109–118.
24. Sun Y, Lee R, Shen K, et al. Structural connectivity analysis reveals topological aberrations in patients with schizophrenia. *Conf Proc IEEE Eng Med Biol Soc*. 2013;2013:1386–1389.
25. Qin J, Wei M, Liu H, et al. Abnormal brain anatomical topological organization of the

cognitive-emotional and the frontoparietal circuitry in major depressive disorder. *Magn Reson Med*. 2014;72(5):1397–1407.
26. Singh MK, Kesler SR, Hadi Hosseini SM, et al. Anomalous gray matter structural networks in major depressive disorder. *Biol Psychiatry*. 2013;74(10):777–785.
27. Zhang J, Wang J, Wu Q, et al. Disrupted brain connectivity networks in drug-naive, first-episode major depressive disorder. *Biol Psychiatry*. 2011;70(4):334–342.
28. Ajilore O, Lamar M, Leow A, et al. Graph theory analysis of cortical-subcortical networks in late-life depression. *Am J Geriatr Psychiatry*. 2014;22(2):195–206.
29. Bai F, Shu N, Yuan Y, et al. Topologically convergent and divergent structural connectivity patterns between patients with remitted geriatric depression and amnestic mild cognitive impairment. *J Neurosci*. 2012;32(12):4307–4318.
30. Bohr IJ, Kenny E, Blamire A, et al. Resting-state functional connectivity in late-life depression: higher global connectivity and more long distance connections. *Front Psychiatry*. 2012;3:116.
31. Lim HK, Jung WS, Aizenstein HJ. Aberrant topographical organization in gray matter structural network in late life depression: a graph theoretical analysis. *Int Psychogeriatr*. 2013;25(12):1929–1940.
32. Barzotti T, Gargiulo A, Marotta MG, et al. Correlation between cognitive impairment and the Rey auditory-verbal learning test in a population with Alzheimer disease. *Arch Gerontol Geriatr Suppl*. 2004;38(9):57–62.
33. Guo Q-H, Chuan-Zhen L, Hong Z. Application of Rey-Osterrieth complex figure test in Chinese normal old people. *Chin J Clin Psychol*. 2000;8(4):205–207.
34. Libon DJ, Malamut BL, Swenson R, et al. Further analyses of clock drawings among demented and nondemented older subjects. *Arch Clin Neuropsychol*. 1996;11(3):193–205.
35. Gordon NG. The Trail Making Test in neuropsychological diagnosis. *J Clin Psychol*. 1972;28(2):167–169.
36. Wechsler D. *WAIS-R manual: Wechsler adult intelligence scale-revised*. New York, NY: Psychological Corp; 1981.
37. Smith A. *Symbol digit modalities test: Manual*. Torrance, CA: Western Psychological Corp; 2002.
38. Watts DJ, Strogatz SH. Collective dynamics of 'small-world' networks. *Nature*. 1998;393(6684):440–442.
39. Latora V, Marchiori M. Efficient behavior of small-world networks. *Phys Rev Lett*. 2001;87(19):198701.
40. Achard S, Bullmore E. Efficiency and cost of economical brain functional networks. *PLOS Comput Biol*. 2007;3(2):e17.
41. Rubinov M, Sporns O. Complex network measures of brain connectivity: uses and interpretations. *Neuroimage*. 2010;52(3):1059–1069.
42. Sexton CE, McDermott L, Kalu UG, et al. Exploring the pattern and neural correlates of neuropsychological impairment in late-life depression. *Psychol Med*. 2012;42(6):1195–1202.
43. Herrmann LL, Goodwin GM, Ebmeier KP. The cognitive neuropsychology of depression in the elderly. *Psychol Med*. 2007;37(12):1693–1702.
44. Bullmore ET, Suckling J, Overmeyer S, et al. Global, voxel, and cluster tests, by theory and permutation, for a difference between two groups of structural MR images of the brain. *IEEE Trans Med Imaging*. 1999;18(1):32–42.
45. Hamilton M. A rating scale for depression. *J Neurol Neurosurg Psychiatry*. 1960;23(1):56–62.
46. Katzman R, Zhang MY, Ouang-Ya-Qu, et al. A Chinese version of the Mini-Mental State Examination; impact of illiteracy in a Shanghai dementia survey. *J Clin Epidemiol*. 1988;41(10):971–978.
47. Bhalla RK, Butters MA, Mulsant BH, et al. Persistence of neuropsychologic deficits in the remitted state of late-life depression. *Am J Geriatr Psychiatry*. 2006;14(5):419–427.
48. Butters MA, Becker JT, Nebes RD, et al. Changes in cognitive functioning following treatment of late-life depression. *Am J Psychiatry*. 2000;157(12):1949–1954.
49. Köhler S, Thomas AJ, Barnett NA, et al. The pattern and course of cognitive impairment in late-life depression. *Psychol Med*. 2010;40(4):591–602.
50. Devanand DP, Pelton GH, Marston K, et al. Sertraline treatment of elderly patients with depression and cognitive impairment. *Int J Geriatr Psychiatry*. 2003;18(2):123–130.
51. Nebes RD, Pollock BG, Houck PR, et al. Persistence of cognitive impairment in geriatric patients following antidepressant treatment: a randomized, double-blind clinical trial with nortriptyline and paroxetine. *J Psychiatr Res*. 2003;37(2):99–108.
52. Tononi G, Edelman GM, Sporns O. Complexity and coherency: integrating information in the brain. *Trends Cogn Sci*. 1998;2(12):474–484.
53. Stam CJ, van Straaten EC. The organization of physiological brain networks. *Clin Neurophysiol*. 2012;123(6):1067–1087.
54. Sporns O, Zwi JD. The small world of the cerebral cortex. *Neuroinformatics*. 2004;2(2):145–162.
55. Yuan Y, Hou Z, Zhang Z, et al. Abnormal integrity of long association fiber tracts is associated with cognitive deficits in patients with remitted geriatric depression: a cross-sectional, case-control study. *J Clin Psychiatry*. 2010;71(10):1386–1390.
56. Shu H, Yuan Y, Xie C, et al. Imbalanced hippocampal functional networks associated with remitted geriatric depression and apolipoprotein E ε4 allele in nondemented elderly: a preliminary study. *J Affect Disord*. 2014;164:5–13.
57. Butters MA, Whyte EM, Nebes RD, et al. The nature and determinants of neuropsychological functioning in late-life depression. *Arch Gen Psychiatry*. 2004;61(6):587–595.
58. Alexopoulos GS, Kiosses DN, Choi SJ, et al. Frontal white matter microstructure and treatment response of late-life depression: a preliminary study. *Am J Psychiatry*. 2002;159(11):1929–1932.
59. Hickie I, Scott E, Wilhelm K, et al. Subcortical hyperintensities on magnetic resonance imaging in patients with severe depression—a longitudinal evaluation. *Biol Psychiatry*. 1997;42(5):367–374.
60. Kumar A, Thomas A, Lavretsky H, et al. Frontal white matter biochemical abnormalities in late-life major depression detected with proton magnetic resonance spectroscopy. *Am J Psychiatry*. 2002;159(4):630–636.
61. Wen MC, Steffens DC, Chen MK, et al. Diffusion tensor imaging studies in late-life depression: systematic review and meta-analysis. *Int J Geriatr Psychiatry*. 2014;29(12):1173–1184.
62. Yuan Y, Zhang Z, Bai F, et al. Abnormal neural activity in the patients with remitted geriatric depression: a resting-state functional magnetic resonance imaging study. *J Affect Disord*. 2008;111(2–3):145–152.
63. Abe O, Yamasue H, Kasai K, et al. Voxel-based analyses of gray/white matter volume and diffusion tensor data in major depression. *Psychiatry Res*. 2010;181(1):64–70.
64. Grieve SM, Korgaonkar MS, Koslow SH, et al. Widespread reductions in gray matter volume in depression. *Neuroimage Clin*. 2013;3:332–339.
65. Guo H, Cao X, Liu Z, et al. Machine learning classifier using abnormal brain network topological metrics in major depressive disorder. *Neuroreport*. 2012;23(17):1006–1011.

Editor's Note: We encourage authors to submit papers for consideration as a part of our Focus on Geriatric Psychiatry section. Please contact Helen Lavretsky, MD, MS, at hlavretsky@psychiatrist.com, or Gary W. Small, MD, at gsmall@psychiatrist.com.

See supplementary material for this article at PSYCHIATRIST.COM.

THE JOURNAL OF CLINICAL PSYCHIATRY
THE OFFICIAL JOURNAL OF THE AMERICAN SOCIETY OF CLINICAL PSYCHOPHARMACOLOGY

Supplementary Material

Article Title: Altered Topological Patterns of Brain Networks in Remitted Late-Onset Depression:A Resting-State fMRI Study

Author(s): Zan Wang, MD; Yonggui Yuan, MD, PhD; Feng Bai, MD; Jiayong You, MD; and Zhijun Zhang, MD, PhD

DOI Number: dx.doi.org/10.4088/JCP.14m09344

List of Supplementary Material for the article

1. eAppendix 1 Supplemental METHOD
2. eTable 1 Cortical and Subcortical Regions of Interest Defined in the Study
3. eTable 2 Raw Scores of Neuropsychological Tests
4. eFigure 1 A Flowchart for The Construction of Functional Brain Networks
5. eFigure 2 Scatter Plots of Topological Properties (Both Global and Regional Metrics) and Neuropsychological Scores in rLOD Patients

Disclaimer

This Supplementary Material has been provided by the author(s) as an enhancement to the published article. It has been approved by peer review; however, it has undergone neither editing nor formatting by in-house editorial staff. The material is presented in the manner supplied by the author.

Altered Topological Patterns of Brain Networks in Remitted Late-onset Depression: A Resting-State fMRI Study

eAppendix 1

Supplemental METHOD

Participants

All rLOD patients met the following inclusion criteria: (1) they had previously met the major depression disorder in DSM-IV criteria and remitted for more than 6 months before the enrollment; (2) the age of first depressive onset was over 60 years; (3) Hamilton Depression Rating Scale (HDRS) scores were lower than 7, and Mini-Mental State Examination (MMSE) scores were higher than 24; (4) duration of illness must be less than 5 years and a medication-free period for all patients was longer than 3 months prior to the assessment; (5) absence of other major psychiatric disorder, including hidden abuse or dependence of psychoactive substances; (6) absence of primary neurological illness, including dementia or stroke; (7) absence of medical illness impairing cognitive function; (8) no history of electroconvulsive therapy; (9) no gross structural abnormalities on T1-weight images, and no major white matter changes such as infarction or other vascular lesions on T2-weight MRI.

Imaging Acquisition

All subjects were scanned using a General Electric 1.5 Tesla scanner (General Electric Medical Systems, USA) with a homogeneous birdcage head coil. Axial R-fMRI (no cognitive tasks were performed, eyes were closed, and ears were occluded) datasets were obtained in seven minutes and six seconds with a single-shot gradient-recalled echo-planar imaging (GRE-EPI) sequence: TR =

3000 ms; TE = 40 ms; FA = 90°; acquisition matrix = 64 × 64; FOV = 240 mm × 240 mm; thickness = 4.0 mm; gap = 0mm and 3.75 mm × 3.75 mm in-plane resolution.

Imaging Preprocessing

Imaging preprocessing was carried out using the Statistical Parametric Mapping (SPM8, http://www.fil.ion.ucl.ac.uk/spm) and Data Processing Assistant for Resting-State fMRI (DPARSF, http://www.restfmri.net/forum /dparsf). The first ten volumes were discarded for scanner stabilization and participants' adaption to the circumstances. The remaining images were corrected for timing differences and motion effects. Participants with head motion more than 3mm maximum displacement in any direction of *x*, *y* and *z* or 3 degree of any angular motion were excluded. Subsequently, the resulting images were spatially normalized into the stereotaxic space using an optimum, 12-parameter affine transformation and nonlinear deformation, and then resampled to 3 × 3 × 3 mm^3 voxels. Further preprocessing included linear detrend and temporal band-pass filtering (0.01-0.1Hz), which were used to reduce the effects of low-frequency drift and high frequency physiological respiratory and cardiac noise. Finally, the nuisance signals involving six head motion parameters, global mean signal, cerebrospinal fluid signal, and white matter signal were regressed out from the data.

Network Construction

To construct the brain functional network, the images of each brain were first parcellated into 90 regions of interest (ROIs, Supplementary eTable 1) using the automated anatomically labeling atlas, which has been broadly used in several previous brain network studies[1-3]. Then the representative time series of each ROI were obtained by simply averaging the fMRI time series over all voxels in this region. Pearson correlation coefficients between each pair of 90 ROIs were subsequently

calculated, thus generating a 90 × 90 correlation matrix for each subject. To avoid complicated statistical descriptions in the following network analysis, our graph theoretical analysis is confined to a simple undirected and unweighted binary matrix (Supplementary eFigure 1). Each absolute correlation matrix was thresholded into a binary matrix with a fixed sparsity level, *S* (defined as the number of edges in a graph divided by the maximum possible number of edges of the graph). Setting a sparsity threshold ensured that all the resultant networks had the same number of edges[3, 4]. As there is no gold standard for a single threshold, we thresholded each absolute correlation matrix repeatedly over a wide range of sparsity levels ($10\% \leq S \leq 34\%$) at an interval of 0.01, and calculated the parameters of the resulting graphs with different thresholds.

Network Analysis

Small-world Parameters

The small-world parameters of a network (clustering coefficient C_p, and characteristic path length L_p) were originally proposed by Watts and Strogatz[5]. Briefly, the C_p of a network is the average of the clustering coefficients over all nodes, where the clustering coefficient C_i of a node is defined as the ratio of the number of existing connections among the node's neighbors and all their possible connections. C_p quantifies the local interconnectivity of a network. L_p of a network is the shortest path length (numbers of edges) required to transfer from one node to another averaged over all pairs of nodes. L_p indicates the overall routing efficiency of a network. To estimate the small-world properties, we scaled C_p and L_p derived from the brain networks with the mean C_p^{rand} and L_p^{rand} of 100 random networks (i.e., $\gamma = C_p / C_p^{rand}$ and $\lambda = L_p / L_p^{rand}$) that preserved the same number of nodes, edges and degree distributions as the real networks[6]. A small-world network should fulfill the conditions of $\gamma > 1$ and $\lambda \approx 1$[5], and therefore, the small-worldness scalar $\sigma = \gamma / \lambda$ will be more than

1[7].

Network Efficiency

The global efficiency measures the ability of parallel information transmission over the network[8]. For a network *G* with *N* nodes and *K* edges, the global efficiency of *G* can be computed as:

$$E_{glob}(G) = \frac{1}{N(N\text{-}1)} \sum_{i \neq j \in G} \frac{1}{L_{ij}},$$

where L_{ij} is the shortest path length between node *i* and node *j* in *G*.

The local efficiency measures the fault tolerance of the network, indicating the capability of information exchange for each subgraph when the index node is eliminated. The local efficiency of *G* is measured as:

$$E_{loc}(G) = \frac{1}{N} \sum_{i \in G} E_{glob}(G_i),$$

where G_i denotes the subgraph composed of the nearest neighbors of node *i*.

Regional Nodal Characteristics

To evaluate the roles of brain regions (or nodes) in brain networks, we computed the regional efficiency $E_{nodal}(i)$[4]. Nodal efficiency measures the information propagation ability of a node with the rest of nodes in the network. The nodal efficiency of node *i* is computed as:

$$E_{nodal}(i) = \frac{1}{N(N\text{-}1)} \sum_{i \neq j \in G} \frac{1}{L_{ij}},$$

where L_{ij} is the shortest path length between node *i* and node *j* in *G*.

Statistical Analysis

Behavioral Data

To increase statistical power by reducing random variability, a composite score analysis was utilized, as previously introduced[9]. First, the raw scores from each test for each subject were

transformed to *z* scores with reference to the means and standard deviations of each test for all subjects. Second, all neuropsychological tests were grouped into four cognitive domains and the related composite scores were calculated by averaging the *z* scores of the individual tests according to the following divisions: Episodic Memory (two test, including AVLT-DR and CFT-DR), Visuospatial Skills (two tests, including CFT and CDT), Processing Speed (two tests, including SDMT and TMT-A) and Executive Function (two tests, including DST and TMT-B).

Network Metrics

Between-group differences in topological attributes (both global and regional measures) were investigated by nonparametric permutation tests[10]. First, we calculated the between-group difference in the mean value of each network metric. To test the null hypothesis that the observed group differences could occur by chance, we randomly reallocated each subject to one of the two groups and recomputed the mean differences between the two randomized groups. The randomization procedure was repeated 10,000 times, and a randomized null distribution based on between-group differences in each metric was created. Then the 95% percentile point of the distribution was used as the critical value for two-tail test of the null hypothesis. This permutation test procedure was repeated at the sparsity of $10\% \leq S \leq 34\%$. In addition, the same permutation procedure was used to compare the AUC of network measures between groups. Of note, before the permutation tests, multiple linear regression analyses were applied to remove the confounding effects of age, gender and years of education for each network metric.

Supplemental REFERENCES

1. Sanz-Arigita EJ, Schoonheim MM, Damoiseaux JS, et al. Loss of 'small-world' networks in Alzheimer's disease: graph analysis of FMRI resting-state functional connectivity. *PloS One* 2010;5(11):e13788.

2. Yao Z, Zhang Y, Lin L, et al. Abnormal cortical networks in mild cognitive impairment and Alzheimer's disease. *PLoS Comput Biol* 2010;6(11):e1001006.

3. Zhang J, Wang J, Wu Q, et al. Disrupted brain connectivity networks in drug-naive, first-episode major depressive disorder. *Biol Psychiatry* 2011;70(4):334-342.

4. Achard S, Bullmore E. Efficiency and cost of economical brain functional networks. *PLoS Comput Biol* 2007;3(2):e17.

5. Watts DJ, Strogatz SH. Collective dynamics of 'small-world' networks. *Nature* 1998;393(6684):440-442.

6. Maslov S, Sneppen K. Specificity and stability in topology of protein networks. *Science* 2002;296(5569):910-913.

7. Humphries MD, Gurney K, Prescott TJ. The brainstem reticular formation is a small-world, not scale-free, network. *Proc Biol Sci* 2006;273(1585):503-511.

8. Latora V, Marchiori M. Efficient behavior of small-world networks. *Phys Rev Lett* 2001;87(19):198701.

9. Sexton CE, McDermott L, Kalu UG, et al. Exploring the pattern and neural correlates of neuropsychological impairment in late-life depression. *Psychol Med* 2012;42(6):1195-1202.

10. Bullmore ET, Suckling J, Overmeyer S, Rabe-Hesketh S, Taylor E, Brammer MJ. Global, voxel, and cluster tests, by theory and permutation, for a difference between two groups of structural MR images of the brain. *IEEE Trans Med Imaging* 1999;18(1):32-42.

Supplementary eTable 1 Cortical and Subcortical Regions of Interest Defined in the Study

Index	Regions	Abbreviation	Index	Regions	Abbreviation
(1,2)	Precentral gyrus	PreCG	(47,48)	Lingual gyrus	LING
(3,4)	Superior frontal gyrus, dorsolatera	SFGdor	(49,50)	Superior occipital gyrus	SOG
(5,6)	Superior frontal gyrus, orbital part	ORBsup	(51,52)	Middle occipital gyrus	MOG
(7,8)	Middle frontal gyrus	MFG	(53,54)	Inferior occipital gyrus	IOG
(9,10)	Middle frontal gyrus, orbital part	ORBmid	(55,56)	Fusiform gyrus	FFG
(11,12)	Inferior frontal gyrus, opercular pa	IFGoperc	(57,58)	Postcentral gyrus	PoCG
(13,14)	Inferior frontal gyrus, triangular pa	IFGtriang	(59,60)	Superior parietal gyrus	SPG
(15,16)	Inferior frontal gyrus, orbital part	ORBinf	(61,62)	Inferior parietal, but supramarginal and angular gy	IPL
(17,18)	Rolandic operculum	ROL	(63,64)	Supramarginal gyrus	SMG
(19,20)	Supplementary motor area	SMA	(65,66)	Angular gyrus	ANG
(21,22)	Olfactory cortex	OLF	(67,68)	Precuneus	PCUN
(23,24)	Superior frontal gyrus, medial	SFGmed	(69,70)	Paracentral lobule	PCL
(25,26)	Superior frontal gyrus, medial orbi	ORBsupmed	(71,72)	Caudate nucleus	CAU
(27,28)	Gyrus rectus	REC	(73,74)	Lenticular nucleus, putamen	PUT
(29,30)	Insula	INS	(75,76)	Lenticular nucleus, pallidum	PAL
(31,32)	Anterior cingulate and paracingulate gyri	ACG	(77,78)	Thalamus	THA
(33,34)	Median cingulate and paracingulate gyri	DCG	(79,80)	Heschl gyrus	HES
(35,36)	Posterior cingulate gyrus	PCG	(81,82)	Superior temporal gyrus	STG
(37,38)	Hippocampus	HIP	(83,84)	Temporal pole: superior temporal gyrus	TPOsup
(39,40)	Parahippocampal gyrus	PHG	(85,86)	Middle temporal gyrus	MTG
(41,42)	Amygdala	AMYG	(87,88)	Temporal pole: middle temporal gyrus	TPOmid
(43,44)	Calcarine fissure and surrounding cortex	CAL	(89,90)	Inferior temporal gyrus	ITG
(45,46)	Cuneus	CUN			

Note: The regions are listed according to a prior template obtained from an AAL atlas.

Supplementary eTable 2 Raw Scores of Neuropsychological Tests

Measures	**rLOD** (n=33)	**HC** (n=31)	***P* values**
Episodic memory			
AVLT-DR	6.55 ± 2.37	8.23 ± 1.75	0.001 [a]
CFT-DR	15.47 ± 7.64	16.79 ± 6.55	0.520 [a]
Executive function			
DST	12.48 ± 2.51	13.16 ± 2.08	0.118 [a]
TMT-B (second)	209.42 ± 119.91	132.10 ± 37.26	0.000 [a]
Processing speed			
SDMT	27.36 ± 14.18	35.97 ± 9.85	0.000 [a]
TMT-A (second)	117.30 ± 84.62	67.97 ± 24.77	0.000 [a]
Visuospatial skills			
CFT	30.74 ± 8.36	34.48 ± 1.75	0.003 [a]
CDT	8.27 ± 2.14	8.97 ± 1.02	0.221 [a]

Data are presented as mean (M) ± stand deviation (SD).

Abbreviations: rLOD, remitted late-onset depression; HC, healthy controls; AVLT-DR, auditory verbal learning test-delayed recall; CFT-DR, rey-osterrieth complex figure test-delayed recall; DST, digit span test; TMT, trail-making test; SDMT, symbol digit modalities test; CDT, clock drawing test.

Note: [a] Analysis of covariance (ANCOVA)

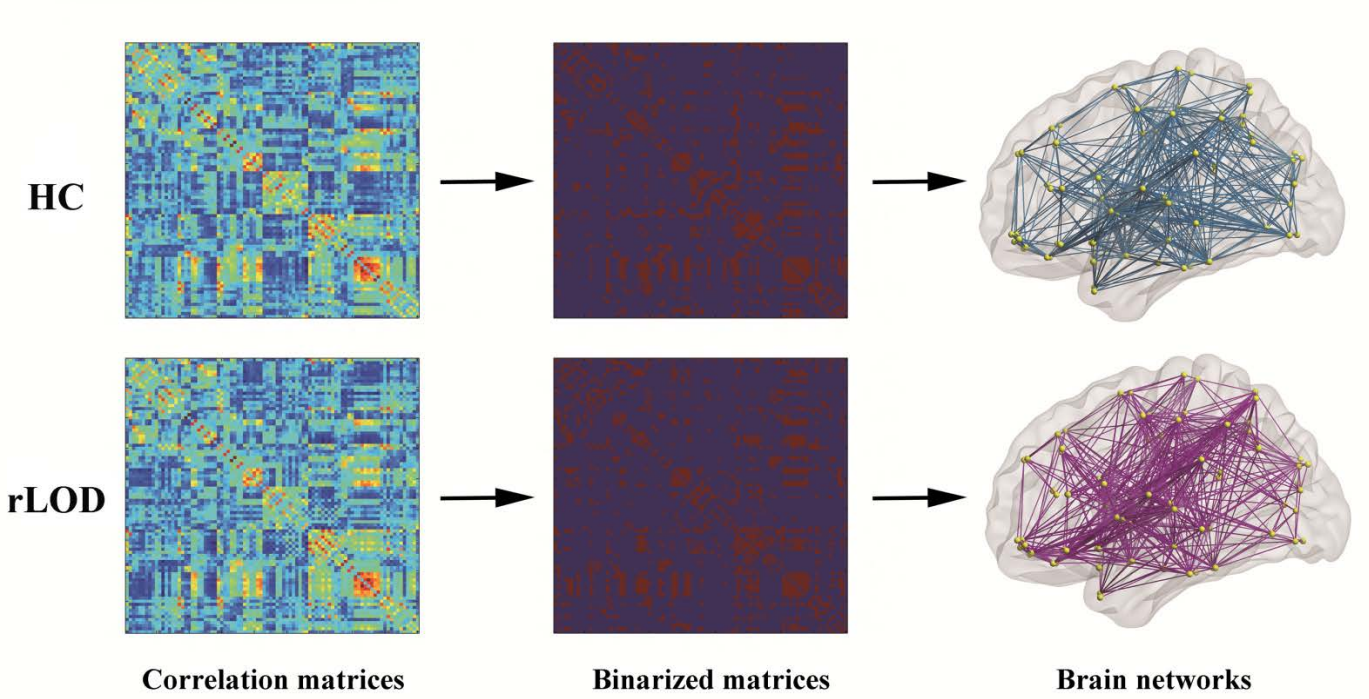

Supplementary eFigure 1 A Flowchart for The Construction of Functional Brain Networks. Left, both in rLOD and HC groups, a correlation matrix was obtained for each subject by calculating inter-regional Pearson correlation coefficient of mean time series among 90 regions; Middle, these correlation matrices were further converted into binarized matrices by applying a thresholding procedure; Right, the obtained binary matrices could be finally represented as networks or graphs that were composed of brain nodes and edges. rLOD, remitted late-onset depression; HC, healthy controls.

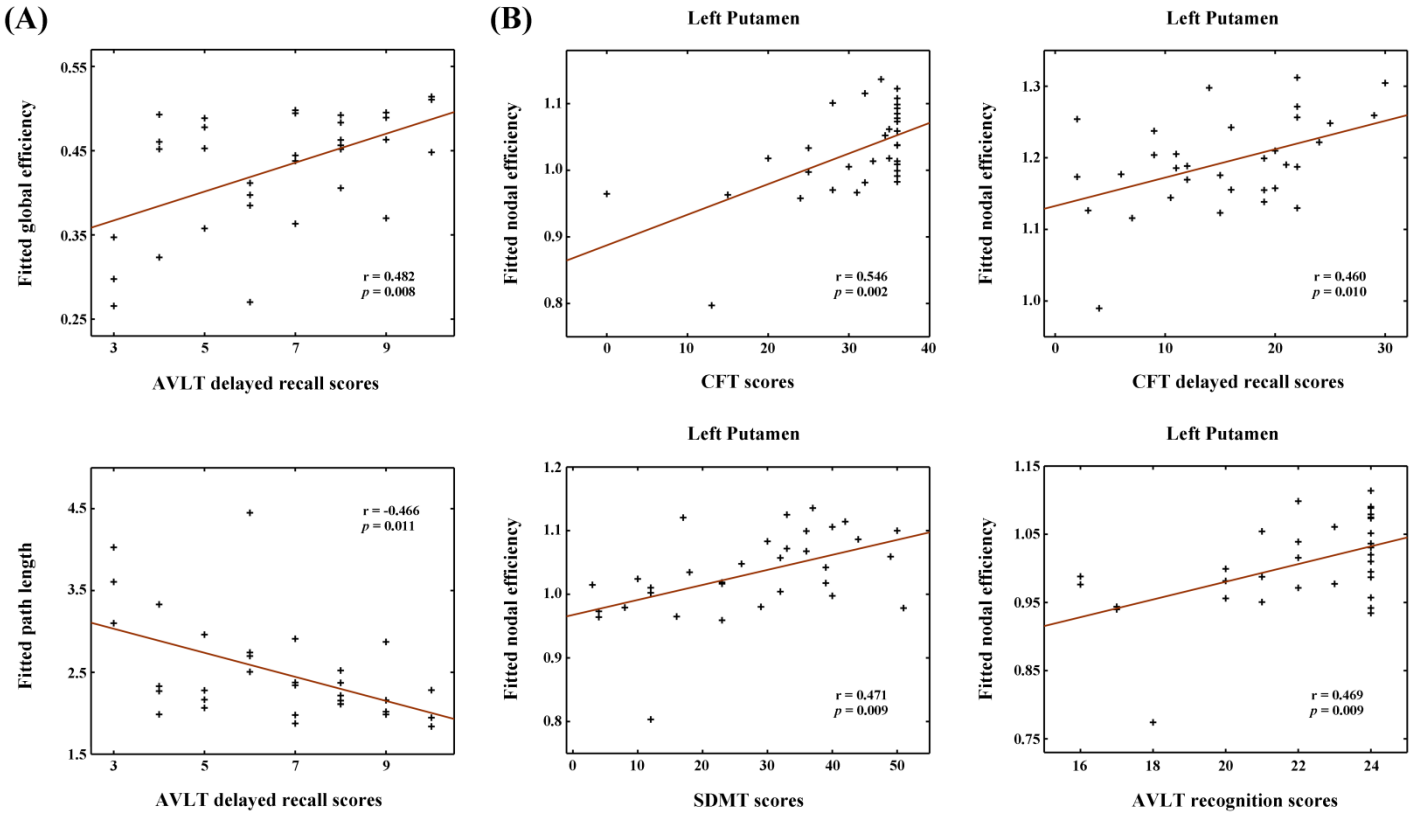

Supplementary eFigure 2 Scatter Plots of Topological Properties (Both Global and Regional Metrics) and Neuropsychological Scores in rLOD Patients. (**A**) The correlations between AVLT-DR scores and L_p and E_{glob}. (**B**) The correlations between nodal efficiency of left putamen and CFT, CFT-DR, SDMT and AVLT-recognition scores. rLOD, remitted late-onset depression; AVLT-DR, auditory verbal learning test-delayed recall; CFT, rey-osterrieth complex figure test; SDMT, symbol digit modalities test.